RSC Advances

This is an *Accepted Manuscript*, which has been through the Royal Society of Chemistry peer review process and has been accepted for publication.

Accepted Manuscripts are published online shortly after acceptance, before technical editing, formatting and proof reading. Using this free service, authors can make their results available to the community, in citable form, before we publish the edited article. This *Accepted Manuscript* will be replaced by the edited, formatted and paginated article as soon as this is available.

You can find more information about *Accepted Manuscripts* in the Information for Authors.

Please note that technical editing may introduce minor changes to the text and/or graphics, which may alter content. The journal's standard Terms & Conditions and the Ethical guidelines still apply. In no event shall the Royal Society of Chemistry be held responsible for any errors or omissions in this *Accepted Manuscript* or any consequences arising from the use of any information it contains.

ROYAL SOCIETY OF CHEMISTRY

www.rsc.org/advances

RSC Advances

RSC Advances

PAPER

Substrate stiffness does affect the fate of human keratinocytes

Prerak Gupta [a], Gautham Hari Narayana S. N. [a], Uvanesh Kasiviswanathan [a], Tarun Agarwal [a,b], Senthilguru K. [a], Devdeep Mukhopadhyay [b], Kunal Pal [a], Supratim Giri [c], Tapas K Maiti [b], Indranil Banerjee [a*]

Received 00th September 2015,
Accepted 00th September 2015

DOI: 10.1039/x0xx00000x

www.rsc.org/

Recent reports on the paradoxical behaviour of epithelial cells in response to the varying stiffness of polydimethyl siloxane (PDMS) substrate has made 'matrix stiffness dependent cellular mechanotransduction' an open issue for further investigation. In this context, we have tried to address the fundamental question, "Are human keratinocytes sensitive towards PDMS substrate stiffness?". To decipher the underlying relationship between PDMS substrate stiffness and keratinocyte mechanotransduction, we modulated the stiffness of the PDMS substrate across a physiological range (elastic modulus ranging from 1.6 MPa to 0.05 MPa) and characterized the behaviour of human skin keratinocytes (HaCaT cells). Priliminary analysis of the topographical features (contact angle, protein adsorption and distribution, and surface roughness) and mechanical properties (elastic modulus, stress relaxation time and ductaility) ensured that all the PDMS substrates were topographically similar but differed in their mechanical properties. Matrix stiffness dependent variation in the cellular response was contoured, qualitatively and quantitatively, by mapping the cytoskeletal organization (FESEM and immunocytochemistry) and studying cell proliferation (live cell population assay, MTT assay in presence and absence of mechanotransduction pathway blockers and flow cytometry analysis of proliferative cell population). Result showed that there was a significant increase in cell proliferation with increasing matrix stiffness whereas cell spreading was affected differentially . Mechanistic analysis revealed that stiffness induced cell proliferation was β-catenin independent but ERK1/2 dependent. Analysis at the nuclear level, showed that the soft surface caused nuclear mechanotransduction (evident from nuclear lamin A/C expression) and perturbed the transcription pattern of protein (VEGF as model protein) in HaCaT cells. The study confirmed that the human keratinocytes are mechanosensitive towards the stiffness of PDMS substrate.

1. Introduction

Substrate stiffness has long been considered as an universal mechano-regulator of adherent cell's physiology [1]. Numerous studies have deciphered the role of substrate stiffness on cellular adhesion [2], migration [3-4], proliferation [5], differentiation [6] and apoptosis (anoikis) [7] of the adherent cells. *In vivo*, the stiffness of various tissues of the human body ranges from few Pascal (Pa) for soft tissues like brain to mega Pascal (MPa) for bone and cartilages [8-9]. Now-a-days, it is a popular understanding that, even *in vitro*, the lineage commitment of the stem cells depends on the matching of substrate stiffness with that of their native tissue stiffness. This notion has been built upon the basis of some elegant examples of tuning the course of stem cell fate *in vitro*, just by altering the stiffness of the cellular niche [10-11]. It has been observed that soft matrices induced neurogenic or adipogenic differentiation, whereas, the harder one supported osteogenic differentiation of human mesenchymal stem cells [10]. However, this much celebrated viewpoint of the matrix stiffness dependent cellular mechanotransduction has recently been contradicted by the two consecutive reports published in 2012 [12] and 2014 [13]. The studies suggested that the bulk stiffness of polydimethyl siloxane (PDMS) substrate did not affect the fate of epidermal stem cells and A549 cells. Trappmann *et al.* proposed that ligand tethering dependent variation in the mechanical feedback resulted in so called 'stiffness induced mechanotransduction [12], while, Li *et al.* argued it to be the interfacial stiffness that is responsible for the variations in the cellular behaviour [13]. In this context, D. J. Mooney's group in 2014 and Ding *et al.* in 2015 published two interesting reports stating that both the matrix stiffness and ligand distribution contribute in a concerted way in the stiffness-dependent mechanotransduction [14-15]. In a recent report, Huang *et al.* showed that the substrate stiffness and the extracellular matrix proteins cooperatively regulate the wound healing in axolotls *in vivo* [16]. From the aforesaid discussion, it becomes evident that the role of matrix stiffness in

[a] Department of Biotechnology & Medical Engineering, National Institute of Technology, Rourkela-769008, Odisha, India.

[b] Department of Biotechnology, Indian Institute of Technology Kharagpur, Kharagpur - 721302, West Bengal, India.

[c] Department of Chemistry, National Institute of Technology, Rourkela-769008, Odisha, India.

* indraniliit@gmail.com; Phone : +91-943-850-7035

† Footnotes relating to the title and/or authors should appear here.
Electronic Supplementary Information (ESI) available: [details of any supplementary information available should be included here]. See DOI: 10.1039/x0xx00000x

This journal is © The Royal Society of Chemistry 2015

RSC Advances Accepted Manuscript

cellular mechanotransduction is still an open issue for further investigation.

So far, a number of substrates has been used to study stiffness-dependent variation in the cellular behaviour including collagen [17], poly(ethylene glycol) [18], polyacrylamide (PAAm) hydrogels [12] and PDMS. A critical review pointed that the contradictory results were obtained when PDMS was used as a preferred substrate. More interestingly, such dubious behaviour of the cells with varying matrix stiffness was observed mostly in the case of cells of epithelial origin. Earlier, various research groups have reported matrix stiffness dependent response of epithelial cells. Saez *et al.* demonstrated a directional growth of epithelial cells in response to the substrate rigidity gradient [19]. A similar response pertaining to the stiffness-dependent wound closure was reported by Anon *et al.* [20]. Recently, Wang *et al.* reported that proliferation, migration and re-epithelisation of HaCaT keratinocytes were favoured on the stiffer substrate, while, it showed adverse effect on cell differentiation [21]. On the contrary, Trepat *et al.* observed that the growth/proliferation of epithelial cell sheet *in vitro* was independent of the substrate stiffness [22]. In lieu of the conventional view, Trappmann *et al.* and Li *et al.* showed that PDMS substrate stiffness had no role in spreading of human epidermal stem cells and A549 (adenocarcinoma human alveolar basal epithelial cells) cells [12-13]. In addition, Zarkoob *et al.* [23] pointed that the average speed of human keratinocytes migration on the soft surface was higher than that of hard surface, contradicting the observation reported by Wang *et al.* [21]. Keeping this controversy in perspective, here, we attempted to resolve the fundamental question, "Are human keratinocytes sensitive towards PDMS substrate stiffness?" This is also a pertinent question in translational biomedical research, wherein, PDMS platforms are frequently used in Lab-on-a-Chip devices for the cell based assay. Therefore, a clear understanding of the influence of PDMS substrate stiffness on the cellular physiology is required.

In this regard, the present report delineates the influence of PDMS stiffness on the behaviour (especially cytoskeletal reorganization and proliferation) of human keratinocytes (HaCaT) cells. During the analysis, effect of different interferential factors like protein adsorption on the matrix surface, surface hydrophobicity and surface roughness were taken into consideration. Unlike the earlier published reports, herein, we have considered the time-dependent variation of visco-elastic parameters of PDMS and correlated them with the cellular behaviour.

2. Materials and Methods

2.1.Materials:

SYLGARD (R) 184 Silicon Elastomer kit was purchased from Dow corning GmbH, Germany. Hydrogen peroxide (30%) and sulfuric acid (98%) were bought from Merck, Mumbai, India. Isopropanol, Dulbecco's Modified Essential Media (DMEM), Dulbecco's Phosphate Buffer Saline (DPBS), Trypsin-EDTA solution, Fetal Bovine Serum (FBS), antibiotic-antimycotic solution and MTT assay kit were purchased from Hi-media, Mumbai, India. Gelatin (type B), paraformaldehyde, triton X-100 and glutaraldehyde were obtained from Sigma-Aldrich, USA. The HaCaT cell line was procured from NCCS, Pune.

2.2.Methods:

2.2.1 Preparation of Polydimethylsiloxane (PDMS) substrate and its surface functionalization

PDMS elastomeric substrates of varying stiffness were prepared by mixing PDMS and curing agent in various proportions (10:1 (P10), 20:1 (P20) and 30:1 (P30) w/w) as described by Goffin *et al.* [24]. The mixtures were degassed and then baked at 65 °C for 3.5 h in hot air oven. Thereafter, the surfaces of the PDMS substrates were treated with piranha solution (98% sulphuric acid and 30% hydrogen peroxide (1:1 v/v)) for 10 min. For all the cell culture experiments, the oxidized PDMS substrates were sterilized under UV light followed by 70% (v/v) ethanol treatment. The surfaces of the PDMS substrates were further coated with sterile 1% (w/v) gelatin (type B) for 30 min at 37 °C prior to cell seeding.

2.2.2 Mechanical Characterization

PDMS substrates were subjected to stress relaxation in a static mechanical tester (TA.HD Texture analyzer, Stable Micro Systems, UK). The stress relaxation studies were conducted by compressing the cylindrical samples (diameter 14.23 mm, height 23.00 mm) to a distance of 2 mm (trigger force: 5 g) and holding the probe at the said distance for 60 sec. For all the experiments, 30 mm flat aluminium probe was used. Percentage stress relaxation (%SR) was calculated using Equation 1.

$$\%SR = \frac{F_0 - F_r}{F_0} \times 100 \quad \text{..... [1]}$$

where, F_0 is the maximum force attained during the compression stage; and F_r is the residual force at the end of the relaxation period.

The viscoelastic parameters of the PDMS substrates were predicted by Weichert model fitting of the stress relaxation data. In this study, the model was created using 3 dashpots, which provides three relaxation times. The mathematical equation (Equation 2) for this model is given below.

$$A = A_0 + A_1.\mathbf{e}^{\left(\frac{-t}{\tau_1}\right)} + A_2.\mathbf{e}^{\left(\frac{-t}{\tau_2}\right)} + A_3.\mathbf{e}^{\left(\frac{-t}{\tau_3}\right)} \quad \text{.....[2]}$$

where, A_0, A_1, A_2 and A_3 are the spring constants; τ_1, τ_2 and τ_3 are time constants of the dashpots and 't' was the time.

2.2.3 Surface characterization of PDMS substrates

The surface of the PDMS substrates was characterized by evaluating the hydrophobicity, protein adsorption and surface

RSC Advances Accepted Manuscript

This journal is © The Royal Society of Chemistry 2015

roughness. The contact angle of PDMS substrates was measured by sessile drop technique (DSA25, Kruss Easy drop) at room temperature (25 °C) in the static mode. For each surface, the contact angle was measured at 10 different spots and expressed as mean ± SD. The protein adsorption on the PDMS substrates was analyzed by checking the absorbance of bovine serum albumin (BSA). In brief, the PDMS substrates were incubated with 1 mg/ml BSA at 37 °C for overnight. Thereafter, the amount of unbound protein was estimated by Bradford assay. The amount of adsorbed protein was estimated indirectly by subtracting the unbound protein from total protein content. Spatial distribution of adsorbed protein on to the PDMS substrates was analyzed by fluoroscence imaging and subsequent image processing using FITC-gelatin as fluoroprobe. For this purpose, gelatin and FITC (1:1 weight ratio) was incubated in bicarbonate buffer (pH 9.2) for 4 h. The reaction was then quenched with 0.01 M ethanolamine and the product was then dialyzed against PBS for 48 h to remove the free FITC. The FITC tagged gelatin molecules (green fluorescent) were allowed to adsorb onto the PDMS surfaces (P10, P20 and P30). All the surfaces were then imaged using a confocal microscope (Olympus fluoview 1000) keeping imaging parameters fixed. Thereafter, the images were subjected for intensity analysis to profile the ligand distribution using NIH ImageJ software. For each substrate 15 random ROIs (region of interest) were selected and data were expressed as mean ± SD. Interfacial surface stiffness of piranha treated PDMS substrates was measured by atomic force microscopy (Model 5500, Agilent, USA. An ethched silicon tip of folowing specification was used for the purpose: cantiliver frequency 150KHz, force constant 40N/m, spring constant 1N/m. The elastic modulus was calculated from load-displacement curve using the software provided by the manufacturer. Surface roughness of gelatin coated PDMS substrates was further analyzed analyzed by atomic force microscopy in non-contact mode All the measurements were performed at room temperature by selecting scanning area range of 10 x 10 μm^2.

2.2.4 Analysis of HaCaT cell morphology on PDMS substrates of varying stiffness.

Adhesion of HaCaT cells to the PDMS substrate of varying stiffness was checked by FESEM and confocal microscopy. For this, HaCaT cells (1 x 10^4 cells/cm^2) were seeded on the gelatin coated PDMS substrates. In general, the cells were maintained in DMEM supplemented with 10 % FBS, 1 % antibiotic-antimycotic solution at 37 °C with regular passaging. For SEM analysis, cells were fixed with 2 % glutaraldehyde, dehydrated with graded ethanol and visualized (FEI, Nova NanoSEM) post gold sputter coating. Quantitative assessments of the cell morphology [cell spreading area and bipolarity index (BI, major to minor axis ratio of cell)] were done by image processing of the confocal micrographs. For this, after 18 h of seeding, the cells were fixed with 4% paraformaldehyde and permeabilized with 0.25 % Triton X100. Thereafter, the actin cytoskeleton and nucleus were stained using TRITC-Phalloidin (Life Technologies, 1:300) and DAPI (Life Technologies, 1:1000) respectively and subjected to confocal microscopy (Olympus fluoview 1000). The images were analyzed using MBF ImageJ software.

2.2.5 Study of cell proliferation and cell cycle analysis

Proliferation studies of HaCaT cells on PDMS substrates of varying stiffness was carried out by both, manual counting of live cells (Trypan blue method) and MTT assay. For this purpose, 3 x 10^4 cells were seeded onto gelatin coated PDMS substrates (P10, P20 and P30) and incubated for 18 h. Then, the spent media containing unadhered cells was discarded from the wells. Cells were then harvested, washed, resuspended in 100 µl of media and subjected for viable cell counting using trypan blue method. The study was carried out in triplicates. The count for each substrate was considered as initial cell number (day 0 count). Cell counting was done for the rest of the wells after 24, 48 and 72 h following the same protocol. The extent of proliferation was measured by subtracting the cell count of two consecutive days ($day_n - day_{(n-1)}$). In addition, MTT assay was also performed for the estimation of cell proliferation following manufacturer's instructions. For that, the substrates were initially seeded with 3 x 10^4 cells/well and incubated for 18 h. To study the direct contribution of matrix stiffness on cell proliferation, specific inhibitors which selectively inhibit the stiffness mediated signal cascade were used. This includes Cytochalasin D (actin destabilizer) and monoethanolate (MEK pathway blocker). In brief, HaCaT cells were first allowed to adhere on PDMS substrate. Thereafter, the cells were treated with different inhibitors [Cytochalasin D (10 µM) for 45 min; Monoethanolate (10 µM) for 30 min]. Proliferation of the cells was assessed by MTT assay post 24 h of the treatment. To validate the results, the percentage of PCNA positive cells in total cell population was also measured by flow cytometry. For this purpose, 5 x 10^5 cells were seeded on PDMS matrix and allowed to adhere for 24 h. Thereafter, the spent media was removed, replaced with fresh media and cells were allowed to grow for another 24 h. Cells were then harvested by trypsinization, fixed with ice-cold ethanol, blocked with 10 % goat serum solution and finally stained with anti-PCNA antibody (primary antibody; mouse anti-human Abcam, 1:100; fluorescence tagged secondary antibody, rabbit anti-mouse 1:100, Abcam, UK). The stained cells were then analyzed by flow cytometer (Accuri C6, BD Biosciences).

2.2.6 Mechanistic analysis of cell proliferation

For the analysis of signalling pathways involved in matrix stiffness induced cell proliferation, we evaluated two most common pathways; namely, Wnt/β-catenin and FAK-ERK pathways. The expression of β-catenin, E-cadherin, and phosphorylated ERK (pERK) in HaCaT cells was analyzed by immunocytochemistry. The cells were cultured on PDMS substrates (P10, P20 and P30) for 72 h. Thereafter, the cells were fixed with standard fixing solutions (4 %

RSC Advances Accepted Manuscript

paraformaldehyde for β-catenin, E-cadherin, and ice-cold methanol pERK 1/2), permealized with 0.25 % Triton X, blocked with 2 % BSA and treated with primary and flurophore conjugated secondary antibodies in sequence. The primary antibodies used for the analysis were mouse anti-human pERK1/2 (1:500, BD Biosciences), rabbit anti-human E-cadherin (1:200, Abcam) and rabbit anti-human β-catenin (1:200, Abcam). Alexafluor 488 donkey anti-rabbit (Life Technologies, 1:500 for E-cadherin & β-catenin) and donkey anti-mouse FITC conjugated (abcam, 1:100 for pERK1/2) were used as secondary antibodies. Actin cytoskeleton and nuclear staining was done using TRITC-phalloidin and DAPI respectively. The samples were imaged by confocal microscope (TCS-SP8, Leica, Germany), keeping imaging parameters same. The image quantification was carried out using MBF ImageJ software. Co-localization of two proteins was quantified by intensity correlation analysis of fluorescence micrographs using intensity correlation analysis (ICA) incorporated in MBF ImageJ. Intensity correlation quotient (ICQ) is an indicator of co-localization, fitted to a scale of − 0.5 for complete segregation, 0.0 for randomness, and + 0.5 for complete colocalization [25].

2.2.7. Study of nuclear mechanotransduction

To confirm the propagation of the stiffness dependent mechanical signal to the cell nucleus and subsequent nuclear mechanotransduction, we evaluated the variation in the expression of nuclear lamin A/C and VEGF. VEGF was chosen as a model protein whose synthesis got typically affted by the alteration in the transcription at nucleus. Expression of nuclear lamin A/C was measured by immunocytochemistry following protocol mentioned above. For this, anti-human lamin A/C (1:400, BD BioScience) and donkey anti-mouse FITC conjugated (1:100, abcam) were used as primary and secondary antibodies respectively. *In vitro* release of VEGF was quantified by ELISA using human VEGF ELISA kit (Abcam 100662). HaCaT cells (1×10^5 cells/well) were seeded on PDMS substrates and cultured for 48 h. The media volume was kept 600 µl to avoid dilution of VEGF. After 48 h of incubation, 100 µl of supernatant was used for the analysis following the protocol provided by the manufacturer.

2.2.8 Statistical Analysis

Each experiment was performed in triplicates and data was reported as mean ± standard deviation (SD). One way ANOVA (analysis of variance) was performed to determine the significant difference between experimental groups p-value was calculated at both 95 and 99 % confidence interval.

3. Results and Discussions

3.1 Mechanical properties

Mechanical properties of PDMS formulations (with different crosslinker : polymer base ratio) has been well documented by various research groups [26-27]. PDMS formulations are viscoelastic in nature and earlier studies mentioned an increase in the mechanical properties like stiffness of PDMS formulation with increasing crosslinker:base ratio. The tuning of stiffness of PDMS substrate by varying the crosslinker:base ratio has been adopted in most of the stiffness dependent studies. However, in a recent report, scientists have shown that cellular mechanotransduction was also governed by non-linear mechanical properties like stress relaxation [28]. Therefore, in the present study the mechanical properties of the samples were analyzed under compression followed by stress relaxation (Fig. 1A). Here, the maximum force obtained during the compression (firmness of the material) was regarded as F_0. After attaining a specified distance, the probe was allowed to stay at the same position for a period of 60 sec. During this time, the force exponentially decreases to a residual force and was regarded as F_R. Such decrease in the force (stress relaxation) could be a result of a combination of molecular rearrangement within the polymer chains, disruption of polymer-polymer interactions and polymer chain breakage [29]. Study showed that (Table 1) there was an increase in the firmness from 124.82 ± 2.01 g-force (P30) to 3684 ± 35.28 g-force (P10) with an increase in the crosslinker proportion from 30:1 to 10:1. The elastic modulus of P10, P20, and P30 was calculated from the stress relaxation profiles and found to be 1.6 ± 0.09, 0.31 ± 0.026 and 0.05 ± 0.04 MPa, respectively. This range of stiffness was in accordance with the previously reported value of PDMS substrate of same base: crosslinker ratio [29]. More importantly, this range of stiffness was found wide enough to analyze the stiffness dependent mechanotransduction [9]. An increase in the mechanical stability is generally associated with reduction in the ductility of the polymer matrices. From stress relaxation study, it was observed that with a decrease in crosslinker concentration, there was an increase in ductility (D_{100}). Study also revealed that the residual forces (F_R) developed within the matrices were in the same order as that of the F_0 values. From the F_0 and F_R values, % Stress Relaxation (%SR) was calculated which provide information about the extent of force dissipated during the relaxation process. From the results, it was observed that the %SR was almost same for P10, P20 and P30 ranging between 8-13 %. The modelling of normalized relaxation profile, using Weichert's 3 dashpot-element mechanical model of viscoelasticity (details mentioned in Table 2) revealed that though the % SR was same for all three matrices but instantaneous parameters (A_1 and τ_1) for P30 were significantly lower than that of P10 and P20 (Fig. 1B, 1C, 1D). It is already known that lower the value of instantaneous relaxation time, better is the molecular rearrangement process under stress. Intermediate and delayed relaxation times provide information about the breakage of polymer-polymer interaction and polymer chains respectively. Both the intermediate and delayed relaxation time of P10 and P20 were similar, but significantly higher in case of P30. All together the mechanical analysis implied that with an change in the base:crosslinker ratio from 30:1 to 10:1, there was a decrease in the ductility and the instanteneous force (A_1) along with an increase in the matrix stiffness (Table 1). Therefore, ductility and instantaneous force A_1 needs to be considered while explaining any trend in cellular behaviour linked to matrix properties.

RSC Advances Accepted Manuscript

This journal is © The Royal Society of Chemistry 2015

Please do not adjust margins

Recently Chaudhury et al has shown that stress relaxation property of the substrate also contribute to the cellar behavior in addition to matrix stiffness [28]. Our mechanical analysis (table 1) showed that for all the samples the percentage stress relaxation was within 15% which is not very high and more importantly the residual force (F_R) were of same order to that of maximum force F_0 which imply no significant variation in mechanical properties of the sample during stress relaxation. As the stress relaxation was measured for a fixed time interval for all samples, therefore, a similar percentage stress relaxation implied same rate of relaxation. Eventually, analysis of the trends of parameters pertaining to stress relaxation clearly showed absolute similarity with stiffness trend, so, in this particular case, it was believed that the matrix stiffness was the key mechanical parameters governing the cellular fate.

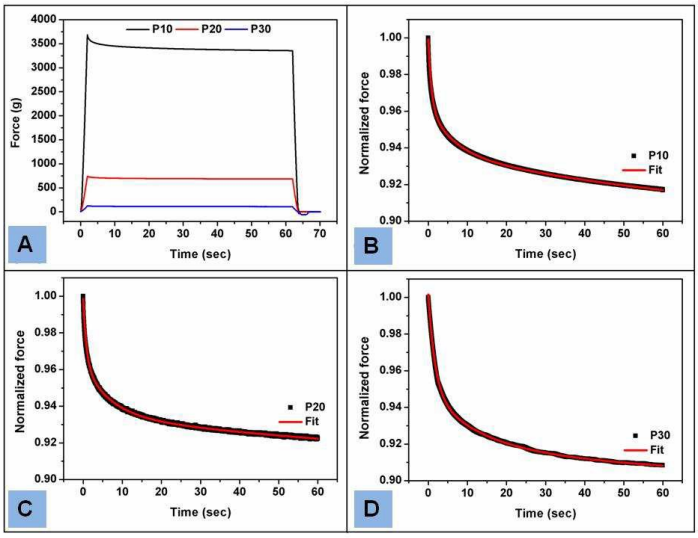

Fig. 1. (A) Stress relaxation profile of PDMS substrates with varying cross linker ratios. Weichert model fitting of the relaxation profile of (B) P10, (C) P20 and (D)P30.

Table 1. Mechanical properties of PDMS substrates of varying base: crosslinker ratio.

Sample	F_0 (g-force)	F_R (g-force)	% Relaxation	D100 (mm)	Ea (MPa)
P10	3684.0 ± 35.28	3353.40 ± 45.91	8.98 ± 0.58	0.23 ± 0.01	1.60 ± 0.09
P20	743.0 ± 62.23	682.98 ± 57.80	8.08 ± 0.31	0.50 ± 0.07	0.31 ± 0.026
P30	124.82 ± 2.01	107.0 ± 2.58	14.21 ± 2.19	1.7 ± 0.03	0.05 ± 0.04

Table 2. Values of instantaneous, intermediate and delayed parameters obtained from Weichert models . A_0, A_1, A_2 and A_3 are the spring constants (normalized value), τ_1, τ_2 and τ_3 are time constants of the dashpots .R^2 is the coefficient of regression.

Weichert Model	P10	P20	P30
A_0	0.886 ± 0.006	0.901 ± 0.003	0.861 ± 0.043
A_1	0.0448 ± 0.003	0.0315 ± 0.002	0.86 ± 0.043
τ_1(sec)	95.42 ± 6.46	104.40 ± 2.39	66.67 ± 4.30
A_2	0.039 ± 0.003	0.0366 ± 0.003	0.0460 ± 0.007
τ_2(sec)	0.808 ± 0.003	0.800 ± 0.030	1.206 ± 0.650
A_3	0.0290 ± 0.37	0.0291 ± 0.002	0.0360 ± 0.009
τ_3(sec)	6.82 ± 0.34	6.65 ± 0.148	7.96 ± 0.477
R^2	0.99	0.99	0.99

RSC Advances Accepted Manuscript

RSC Advances

PAPER

3.2 Surface properties, protein adsorption and distribution on PDMS substrates

Surface hydrophobicity and surface roughness play a very critical role in determining the cell-substrate interaction. These two factors together govern the adsorption and distribution of cell-binding ECM ligands like RGD on the substrate surface. The cell surface receptors such as integrins bind with these ECM ligands which activate a number of signaling cascades. These cascades play an important role in determining the fate of the adherent cells. On the other hand, matrix–stiffness related mechanical signal propagate through the same ECM-integrin ligand-receptor complexes. Therefore, any change in the number or spatial distribution of these ligand-receptor complex could alter the nature or magnitude of mechanical stimuli. So, it becomes an issue of great debate that which factor contribute to what. As mentioned in the introduction section, different research groups are now trying to decouple the chemical cues (ligand distribution) from physical factors (matrix stiffness). A general approach in this regard is to use a nanopattarend cell-binding ligand field on non-adherent substrate of varying mechanical stiffness. Use of ordered array of micropillers has also been explored to address the aforesaid question. Though these systems allow decoupling of chemical cues from matrix stiffness, however, it also restrict the weak secondary cell – material interaction outside the focal adhesion zone which may have significant role in determining cell-fate. In this present study, we did not tried to decouple the surface property from matrix stiffness experimentally but we tried to take in account every aspect of it while drawing inferences. For this purpose, surface hydrophobicity, roughness, total protein adsorption and protein distribution were analyzed in conjugation interfacial stiffness measurement. In this study, piranha treatment is used for oxidation of PDMS. Surface oxidation of PDMS substrate by piranha treatment leads to substitution of methyl groups with –OH to form silanol group, which is highly polar [30] and render the surface hydrophilic. Analysis showed that (Fig. 2A) unoxidized PDMS substrates (P10, P20 and P30) exhibited contact angle around 106° ± 3° whereas after piranha treatment, it reduced to 58° ± 3°, indicating an increase in surface hydrophilicity. These results were in agreement with the previously published reports [27]. Interestingly, as per our expectation, we did not observe any stiffness dependent variation in the contact angle. Another major aspect is to quantify the amount of protein adsorbed and analyzing distribution of adsorbed protein onto PDMS substrates. We observed that adsorption profile of BSA did not follow any linear co-relation with stiffness. Amount of bound protein on oxidized surfaces was 0.027 ± 0.01mg for P10 (stiff substrates) and 0.018 ± 0.003 mg (soft substrates) for P30 (Fig. 2B). No significant difference in protein adsorption was observed among PDMS substrates of varying stiffness ($p > 0.05$). These findings were in accordance with the wettability data. A slight increase in the protein adsorption was observed on oxidized PDMS substrates as compared to unoxidized one, which may be attributed to the improved hydrophilicity. Further, we attempted to analyze the spatial distribution of ligand molecules. Analysis of the confocal images of the PDMS surfaces coated with FITC-gelatin (Fig. 2C) showed that there was no significant difference among ligand distribution ($p > 0.05$). Interfacial stiffness is considered as a contributing parameter in stiffness dependent cellular mechanotransduction. In practice, when PDMS substrates are subjected for plasma oxidation, a thin uniform layer of oxidized PDMS formed at exposed surface which differed markedly from the bulk PDMS in terms of surface properties as well as mechanical properties. AFM data analysis (Fig. 2D) showed that the elastic modulus of P10 was 0.38 ± 0.017 MPa whereas the same for P20 is 0.05 ± 0.007 MPa. We failed to measure the same for P30 because of higher roughness which caused non-uniform indentations across the surface. One noticable point is that, though piranha oxidizes PDMS but unlike plasma treatment, it did not cause formation of uniformly oxidized surface layer; rather, it increased the surface roughness and induce scratches through oxidation. It was observed that roughness increased more for PDMS of low crosslinker ratio (P30). A critical analysis of relative stiffness between P10 and P20 at bulk (table 1) and surface (Fig.2B) revealed a consistancy (Ep10 / Ep20 at bulk = 5.33, Ep10 / Ep20 at surface = 7.5) which justified the rationale of carrying out the experiment on the basis of bulk stiffness. Surface roughness and topography of protein adsorbed surface was examined using AFM. The RMS roughness values for 1% gelatin coated PDMS substrates were found to be 1.88, 1.27 and 1.66 for P10, P20 and P30, respectively (Fig. 2E). Similar to the protein adsorption profiles, no co-relation was observed between surface roughness and substrate stiffness. RMS roughness value for PDMS substrates of different elastic modulus ranged from 1.27-1.88 nm, which is generally not detectable by most cells [31]. Previous studies suggested that surface steps ~11nm are pre-requisite for the occuarance of the contact guidance phenomena [32]. This clearly suggests that topographically all the samples should be recognized by the cells as identical. Ligand tethering is another issue that often needs special attention in stiffness dependent cellular mechanotransduction. However, in recent work, Engler *et al.* [6] showed that PDMS did not support protein tethering, whereas, other substrate like polyacrylamide do. In this context, we also performed microfluidics based wash-off study to confirm that the binding interaction of protein to PDMS substrate is independent of

RSC Advances Accepted Manuscript

the matrix stiffness (for details see Supplementary data 1). In this experiment, the adsorbed FITC-tagged gelatin were exposed to microflow induced shear stress under 'partial slip' flow condition. It is already known that microfluidic shear force can alter the configuration of the matrix bound macromolecules (elongation or bending) [33]. We exploited the same to analyze the quantitative retention of ligands on PDMS matrices of different stiffness after exposing them to microfluidic shear force. Magnitude of varation in fluoroscence intensity before and flow for all three PDMS substrate were found similar. These studies assured that the difference in cellular behavior would be solely influenced by the substrate stiffness.

3.3 Substrate stiffness dependent variation in cell morphology

Spreading of the adherent cells on the basal matrix is very important in the context of cell survival, lineage commitment and differentiation. Initial observation by scanning electron microscope confirmed that cells were adhered properly on the PDMS substrates (Fig. 3A). Well spreaded colony of HaCaT cells were found on all the matrices. A number of studies have shown that the matrix stiffness influence spreading of the cells [5]. As mentioned earlier, recently two groups have shown that spreading of epidermal cells is indifferent to the stiffness of PDMS matrix. Here, the average cell spreading area was found 1751.11 ± 636.33 μm^2 for P10 surface which got reduced to 1412.98 ± 444.55 and 801.88 ± 127.57 μm^2 in case of P20 and P30, respectively (Fig. 3B-C). A change was also observed in the shape factor (bi polarity index, BI). BI value of HaCaT cells were found in the range of 1.33 ± 0.28 to 1.27 ± 0.09 for all the substrates (Fig. 3D). When analyzed critically it was revealed that the variation in cell spreading on P10 and P20 were statistically insignificant but the same between P20 and P30, and P10 and P30 were significant. A similar trend was also observed in case of shape factor calculation. In case of shape factor, statistically significant variation was found between P10 and P30 only. The observed stiffness-independent cell spreading in P10 and P20 were in close accordance to the earlier results reported by Engler *et al.* [6]. It was observed that cell spreading was significantly less in case of P30 in comparison to P10 and P20. We believed that in case of P30, low cell spreading area was not because of the poor mechano-transduction but because of the stickiness of P30 which prevented the spreading of rounded cells mechanically (viscous effect). The consistency in the shape of the adhered cells could probably because of the stiffness-independent uniform distribution of the adhesion ligands (cell binding domail of gelatin molecules) over the PDMS surfaces (Fig. 2C).

3.4 Proliferation of HaCaT cells on PDMS substrates

Preliminary analysis of the cell growth by live cell counting and MTT assay together showed that the stiffer PDMS substrate favored keratinocyte proliferation. Trypan blue based manual live-cell counting assay showed that after 3 days of culture, there was almost a 6.8 fold increase in the cell number in P10, whereas the cell number increased 5.5 and 4.5 folds in P20 and P30, respectively (Fig. 4A). A similar trend was observed in MTT assay. The highest proliferation was observed in P10 (5.5 fold increase in 3 days with respect to 'Day 0' reading) followed by P20 (4.8 fold) and P30 (3.2 fold) (Fig. 4B). Interestingly, it was observed that the rate of cell growth increased with time. Such an increase in the growth rate was found directly related to the matrix stiffness and an increased rate was observed onto stiffer substrates. The stiffness dependent variation in the cell growth was found statistically insignificant during the initial 24 h. However, after the said time period, tha cells started proliferating at different rates on the PDMS matrices of different stiffness. The cell proliferation study was further checked in the presence of cytochalasin D (a microfilament blocker) and U0126 monoethanolate (MEK inhibitor) to ensure the contribution of the matrix stiffness on cell growth (Fig. 4C). It is already known that cells exert traction force to the substrate via actin-myosin network and its corresponding reaction force which is actually the mechanical cues propagate back to the cells through the same cytoskeletal network. Hence, it is believed that destabilization of the cytoskeletal network by microfilament blocker like cytochalasin-D should hinder the stiffness induced signal transduction and subsequent cell proliferation. Our study showed that cytochalasin-D mediated inhibition of cell growth was 65.77 ± 2.1 % in case of P10 whereas the same were 61.61 ± 5.1 and 50 ± 0.9 % for P20 and P30, respectively.

RSC Advances Accepted Manuscript

RSC Advances

PAPER

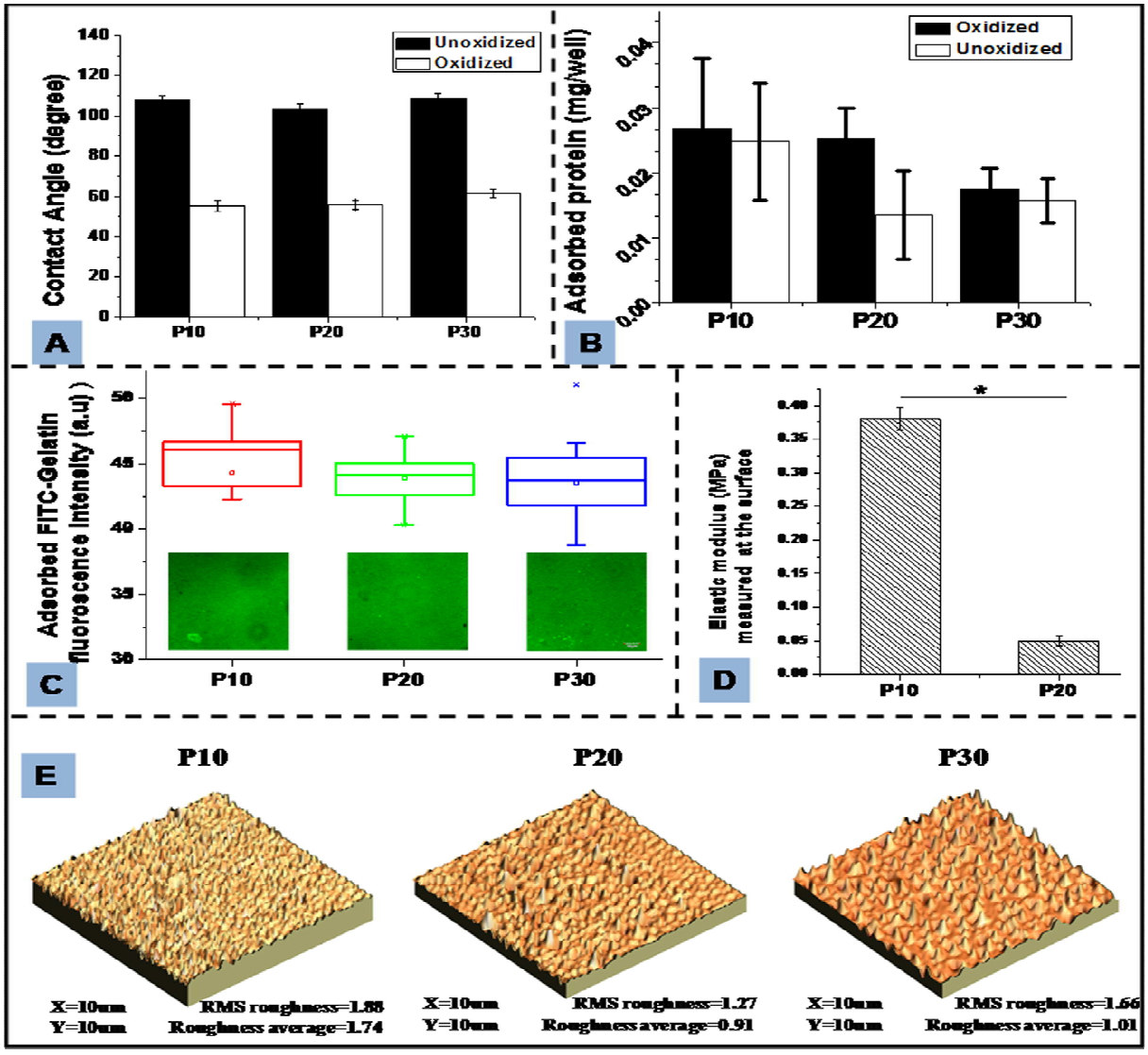

Fig. 2. (A) Contact angle measurement of PDMS substrates before and after oxidation. (B) Protein adsorption on oxidized and unoxidixed PDMS substrates. (C) Analysis of the fluoroscent intensity of adsorbed FITC-gelatin molecules on PDMS surface. For each substrate, 15 random ROI were selected and measured. Data was expressed as Mean ± S.D. Variation in contact angle and protein adsorption and protein distribution were found statistically insignificant among P10, P20 and P30 (p> 0.05). (D) interfacial surface stiffness of piranha treated PDMS substrates (uncoated) were measured by AFM and Elastic modulus obtained from Load-distance curve was plotted. (E) Surface roughness of PDMS substrates was measured by AFM (10x10µm scanning area). Surface was treated with piranha solution and coated with 0.1% gelatin (Type B) prior to imaging.

RSC Advances Accepted Manuscript

Please do not adjust margins

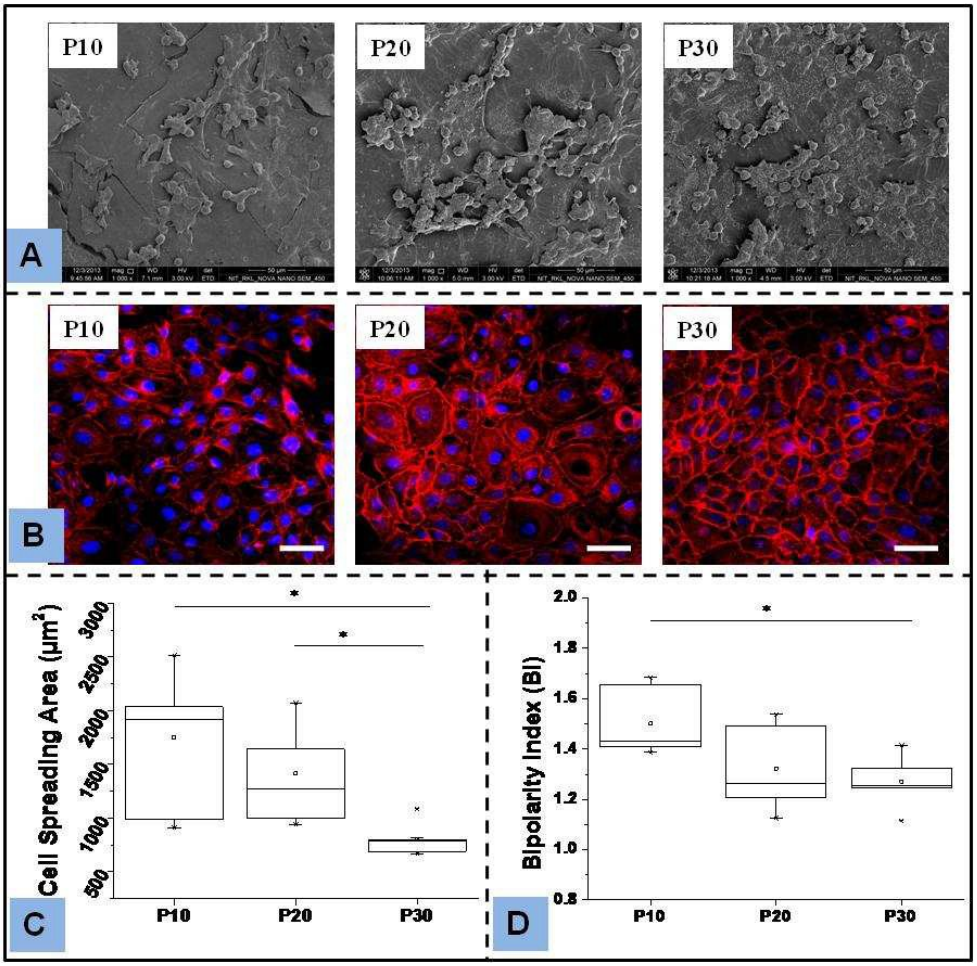

Fig. 3. (A) FE-SEM images of HaCaT cells cultured on PDMS matrices of varying stiffness. (B) HaCaT cell spreading on PDMS substrates of varying stiffness. Cytoskeletal F-actin was stained with TRITC-phalloidin (red) and nucleus was counter stained with DAPI (blue). (C, D) Image analysis of cell spreading. Atleast 5 images were processed to calculate Average cell spreading area and Bipolarity Index (BI). Data were expressed as Mean ± S.D. (*p<0.05, Scale bar 50μm).

respectively. The percentage inhibition of cell growth was found 52.38 ± 3.36, 39.05 ±3.8 , and 26.66 ± 4.7 % for P10, P20, and P30, respectively, when treated with monoethanolate (blocking downstream of mechanotransduction pathway). Such co-relation between matrix stiffness and blocker-induced growth retardation clearly suggest that substrate stiffness directly influenced the cell proliferation. Influence of matrix stiffness on cell proliferation was confirmed by checking the population of PCNA positive cells. PCNA is an evolutionarily well-conserved protein, found in all eukaryotic species and considered as an excellent marker of the proliferative cells. Our flow cytometry based study (Fig. 4D, 4E) showed that proliferative cell population was highest in stiffer matrix. Percentage population of PCNA positive cells was 65.19 ± 0.82 % in P10 substrates whereas the same for P30 was only 21.79 ± 3.69 %. Further, comparison showed that PCNA positive population of P10 was close to that of TCP (70.76 ± 1.35 %). From this, it becomes evident that stiffness of the PDMS substrates greatly influence the proliferation of HaCaT cells. These datas are in accordance with the conventional notion of stiffness dependent cell proliferation.

3.5 Mechanistic analysis of mechanotransduction induced cell proliferation.

Wnt/β-catenin and FAK-ERK pathways are two common signalling cascades that result in matrix stiffness dependent cell proliferation [34-35]. β-catenin was initially known for its involvement in intercellular adhesion structure called adherens junctions. Later, it was realized that β-catenin is a key member in the Wnt signalling pathway. In response to Wnt signals, it translocates to the nucleus and transactivates transcription of target genes together with members of the Tcf/Lef1 transcription factor family [36-37]. However, there are some other reports which contradict this much established view of β-catenin involvement in cell proliferation. Posthaus *et al.* has already showed that β-catenin is

RSC Advances Accepted Manuscript

RSC Advances

PAPER

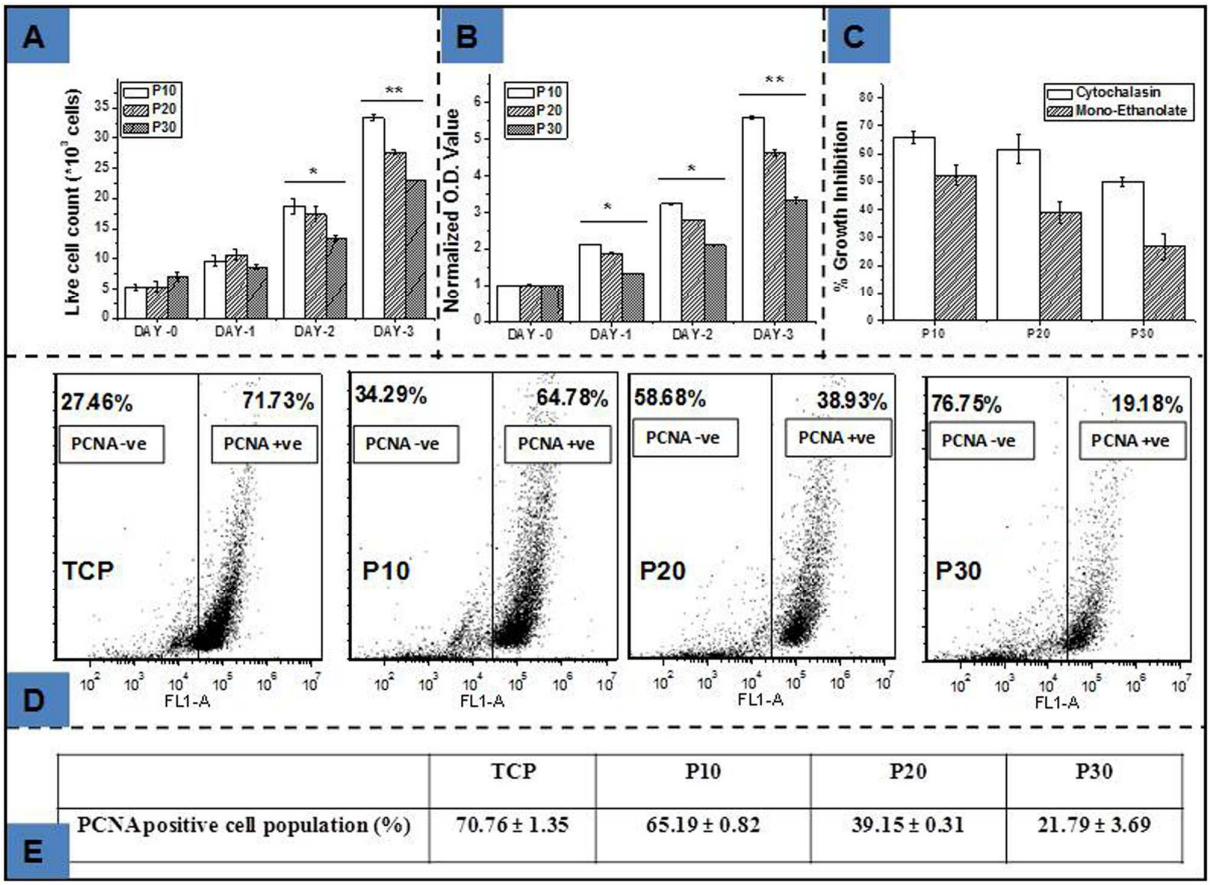

Fig. 4. Analysis of the cell viability and proliferation of HaCaT cells cultured on PDMS substrates of varying stiffness. (A) Trypan blue based live cell counting, (B) Normalized MTT assay values, (C) Growth inhibition profile of HaCaT cells on PDMS substrates in presence of cytochalasin D and Mono-Ethanolate. (D) Representative flow cytometry data of PCNA positive and PCNA negetive cell population on PDMS substrates. (E) Quantitative analysis of percentage population of PCNA positive cells by flow cytometry. Data were expressed as mean ± S.D. Statistical significance was checked for *p<0.05, and **p<0.01. The variation in PCNA positive cell population were found statistically significant (*p<0.05) among all the groups.

RSC Advances Accepted Manuscript

RSC Advances

RSC Advances

PAPER

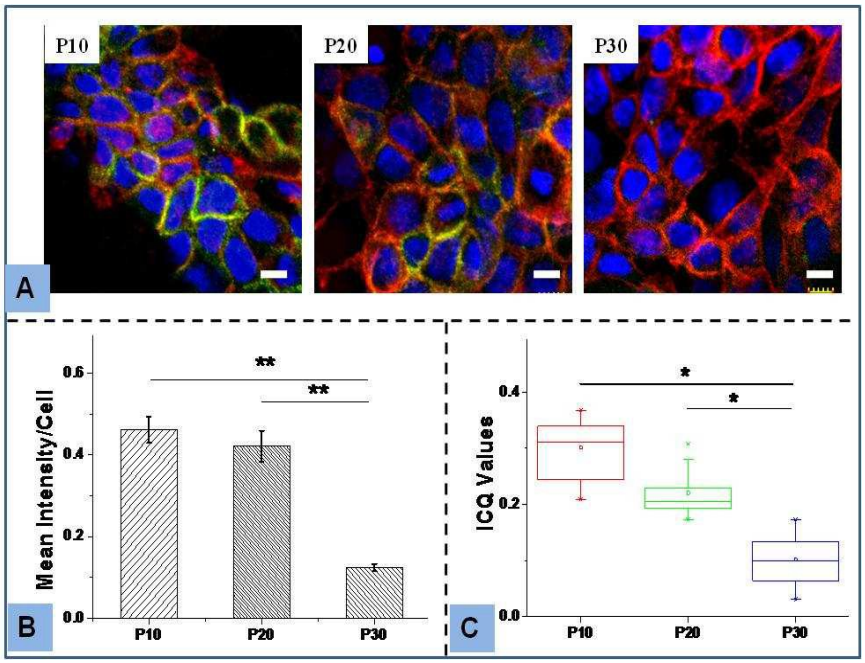

Fig.5. Expression of β-catenin in HaCaT cells cultured on PDMS substrates of varying stiffness. (A) Confocal microscopic images of HaCaT cells stained with FITC tagged anti-β- catenin antibody (green), DAPI for nucleus (blue) and TRITC-phalloidin for actin cytoskeleton (Red). Quantification of β-catenin expression, (B) Mean Intensity and (C) ICQ value. (*p<0.05, **p<0.01, Scale bar 10μm).

not required for proliferation of mouse epidermal keratinocytes [38].

Our study showed that there was a stiffness dependent decrease in the cellular expression of β-catenin in epidermal HaCaT cells (Fig. 5A). Quantitative image analysis showed β-catenin expression decreased 2.5 folds over a change of matrix stiffness from 1.6 MPa (P10) to 51 kPa (P30) (Fig. 5B). However, irrespective of the level of expression, β-catenin was found mostly confined at the cell periphery and not in the nucleus (Fig. 5C). The ICQ value (co-localization) of β-catenin and F-actin was found highest in P10 followed by P20 and P30, respectively. This suggested that though there was a stiffness dependent variation in β-catenin expression but that was probably involved in adheren junction formation, not in cell proliferation. We further checked the cellular expression of E-cadherin which is a cell-cell adhesion molecule. Our study (for details see supplementary data 2) showed that E-cadherins expression (magnitude and spatial distribution) followed the same trend to that of β-catenin. It is well known that at adheren junction, β-catenin binds with the cytoplasmic domain with E cadherins. The similarity in the expression profile between β-catenin and E-cadherin gives a clear indication about its involvement in stiffness dependent cell-cell contact but not in cell proliferation. This observation was found coherent to the existing understanding of epidermal cell physiology. In case of actin-FAK-ERK mechanotransduction pathway, FAK first gets phosphorylated at tyrosine residues 397 and 925 which promote phosphorylation of extracellular signal-regulated kinases 1 and 2 (ERK1/2) and subsequently, cell proliferation [39-40]. We attempted to ascertain whether substrate stiffness induces any alteration in the ERK activation (phosphorylation) and cellular distribution. The pERK1/2 expression in HaCaT cells was found to increase with increasing PDMS stiffness (Fig. 6A). Quantitative image analysis showed that cellular expression of pERK1/2 in P10 was 1.5 fold higher than P20 while the same for P20:P30 is 2:1. All the data were found statistically significant (Fig. 6B). These results were in accordance with the previous published reports [19-21] and favours the general concept of stiffness dependent cellular mechanotransduction.

RSC Advances Accepted Manuscript

3.6 Stiffness induced mechanotransductionat at nuclear level: Study of lamin A/C expression and VEGF secretion

It is already proven that mechanical forces that are exerted on surface-adhesion receptors, such as integrins and cadherins, are also channelled along cytoskeletal filaments and concentrated at distant sites in the cytoplasm and nucleus [41]. Now, it is known that these forces can also cause change in the nuclear size, shape and most importantly gene transcription . To decipher the influence of PDMS substrate stiffness on nuclear mechanotransduction, expression of lamin A/C was studied.

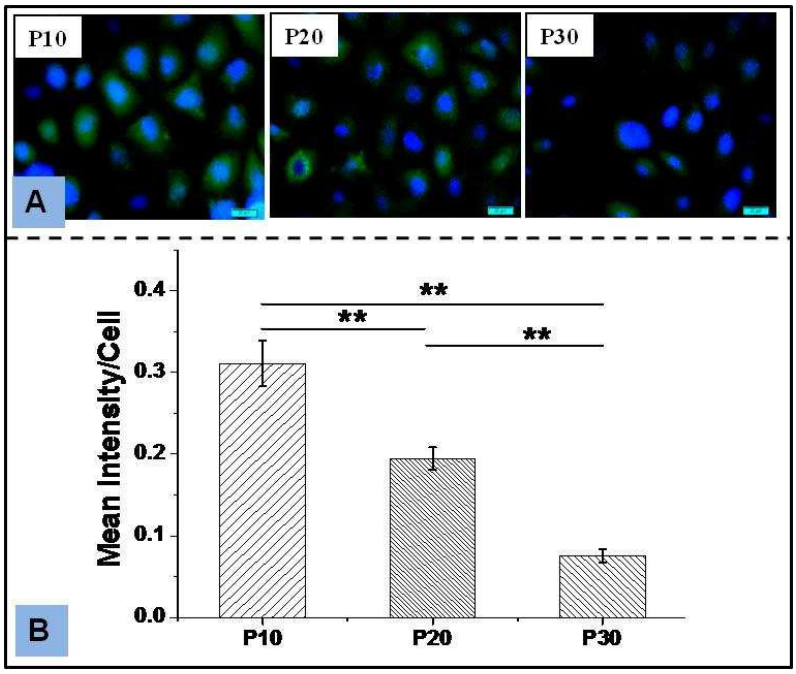

Fig. 6. Expression of pERK1/2 in HaCaT cells cultured on PDMS substrates of varying stiffness. (A) Confocal microscopic images of HaCaT cells stained with FITC tagged anti-pERK1/2 antibody (green) and DAPI for nucleus (blue). (B) Quantification of pERK1/2 expression by calculating mean Intensity. (p<0.01, Scale bar 10µm).**

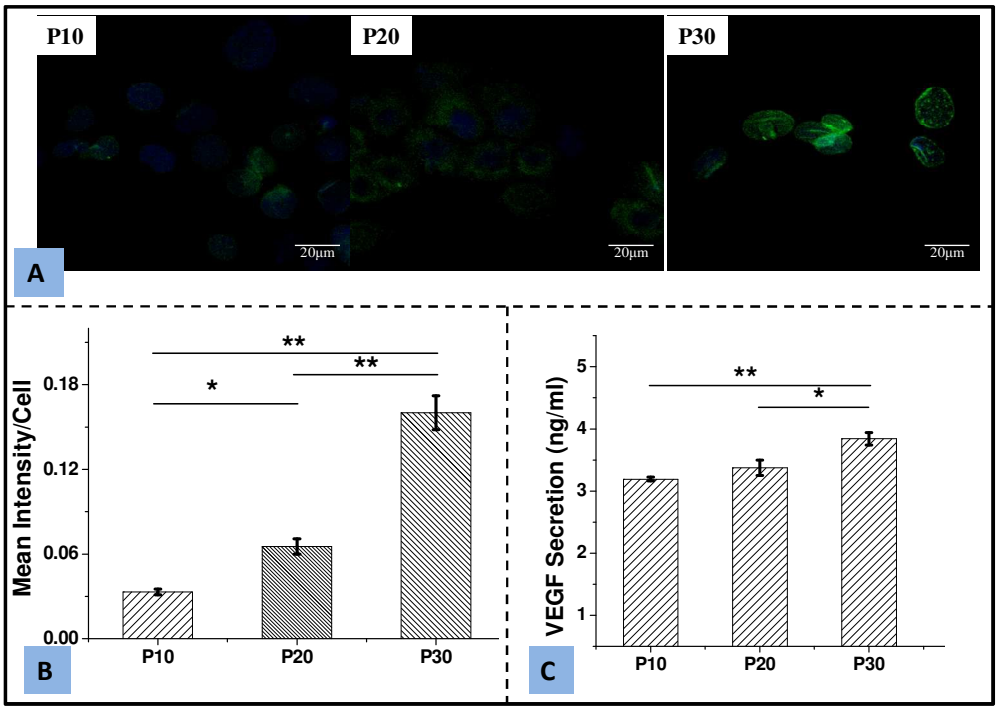

RSC Advances Accepted Manuscript

This journal is © The Royal Society of Chemistry 2015

Please do not adjust margins

Fig. 7. Expression of lamin A/C in HaCaT cell nucleus cultured on PDMS substrates of varying stiffness. (A) Confocal microscopic images of HaCaT cells stained with FITC tagged anti-lamin A/C antibody (green) and DAPI (blue). (B) Quantification of lamin A/C expression by calculating mean Intensity/cell. (C) Analysis of VEGF secretion by HaCaT cells over a period of 48 hours. (*p<0.05,p<0.01).**

Lamins are the main components of the nuclear lamina and form stable structures in the nuclear interior. Lamins A/C are in dynamic equilibrium between the nuclear lamina at the periphery and the nuclear interior. It is believed to modulate gene expression both at the nuclear periphery and interior [42]. It is already established that lamin A/C expression can be correlated to the nuclear mechanotransduction. Our study showed that cellular expression of lamin A/C increased with a decrease in the PDMS stiffness (Fig. 7A). Quantitative image analysis showed that there was a 6 fold increase in lamin A/C expression with the reduction in the substrate stiffness from 1.6 MPa to 0.05 MPa (Fig. 7B). This clearly showed that HaCaT cells are quite sensitive towards PDMS stiffness. It also proved that matrix stiffness induced mechanotransduction in HaCaT cells not only affect the cytosolic signalling but influence the nucleus too. An important point that needs to be mentioned here is that earlier Discher *et al.* [43] showed an increase in Lamin A/C expression with increasing substrate stiffness which seems contradictory to the present findings. This phenomenon could be a characteristic of epidermal cells and more importantly may be associated with absolute value of matrix stiffness. As lamin AC expression is predominantly associated with cell differentiation, so it may happened that P30 was able to induce keratinocyte differentiation because its stiffness is somewhat close to the native skin tissue.

An indirect evidence that favor the argument is that, in most of the cases, increased matrix stiffness favored the cell migration however in case of keratinocytes, migration on softer surface was higher than that on stiffer surface [23]. However, this particular point needs to be investigated further in details We further questioned whether such nuclear mechanotransduction really altered gene transcription or not. For this purpose, we took vascular endothelial growth factor as model protein. Keratinocytes are known secreator of VEGF [44]. Cellular VEGF secretion was generally governed by two transcription factors, namely, HIF-1α and Sp1 [45]. It was hypothesized that if PDMS stiffness-induced nuclear mechanotransduction influence the transcription, then there should be some variation in the VEGF expression level. Our study showed that there was a statistically significant increase in cellular VEGF secretion with a decrease in PDMS stiffness (Fig. 7C). The trend was found similar to that of lamin A/C. Earlier Derricks *et. al*., reported that endothelial cells on soft surface was more responsive towards VEGF than cells cultured on hard surface [46]. Our result suggested that variation in PDMS stiffness lead to variation at gene transcription in HaCaT cells.

5. Conclusion

In the present study, we have tried to address the recent controversy over the behavior of epithelial cells cultured on the PDMS substrate. For this purpose, human keratinocyte cells were cultured on topographically similar PDMS substrate of different stiffnesses. The study suggested that the stiffer matrix supported spreading and proliferation of the HaCaT cells. The variation in the matrix stiffness resulted in the modulation of Wnt/β-catenin and FAK-ERK pathways, known to influence cell-cell adhesion and proliferation. Stiffer matrix induced higher expression of β-catenin and ERK1/2 in HaCaT cells. Furthermore, the study revealed that the stiffness induced mechanical signal reached to nucleus and caused nuclear mechanotransduction. The substrates of lower stiffness supported the expression of nuclear lamin A/C . The study confirms that the variation in the stiffness of the PDMS substrates results in modulation in the morphology, proliferation and signal cascades in HaCaT cells. This observations are inaggrement with the conventional notion of stiffness dependent cellular mechanotransduction.

6. Acknowledgement:

Authors acknowledge Department of Biotechnology (DBT), Govt of India (RGYI scheme project no. BT/PR6227/GBD/27/390/2012).
Authors would like to thank Prof. K.Pramanik and Prof. A. Thirugnanam for providing confocal microscopy facility and contact angle measurement facility.

7. References:

1. R. J. Pelham and Y.-L. Wang, *Proceedings of the National Academy of Sciences*, 1997, **94**, 13661-13665.
2. T. Yeung, P. C. Georges, L. A. Flanagan, B. Marg, M. Ortiz, M. Funaki, N. Zahir, W. Ming, V. Weaver and P. A. Janmey, *Cell motility and the cytoskeleton*, 2005, **60**, 24-34.
3. C.-M. Lo, H.-B. Wang, M. Dembo and Y.-l. Wang, *Biophysical journal*, 2000, **79**, 144-152.
4. M. R. Ng, A. Besser, G. Danuser and J. S. Brugge, *The Journal of Cell Biology*, 2012, **199**, 545-563.
5. J. D. Mih, A. Marinkovic, F. Liu, A. S. Sharif and D. J. Tschumperlin, *Journal of Cell Science*, 2012, **125**, 5974-5983.
6. J. H. Wen, L. G. Vincent, A. Fuhrmann, Y. S. Choi, K. C. Hribar, H. Taylor-Weiner, S. Chen and A. J. Engler, *Nature materials*, 2014.
7. Z. Ma, Z. Liu, D. P. Myers and L. S. Terada, *Cell Cycle*, 2008, **7**, 2462-2465.

RSC Advances Accepted Manuscript

8. A. J. Engler, M. A. Griffin, S. Sen, C. G. Bönnemann, H. L. Sweeney and D. E. Discher, *The Journal of Cell Biology*, 2004, **166**, 877-887.
9. P. C. Georges, W. J. Miller, D. F. Meaney, E. S. Sawyer and P. A. Janmey, *Biophysical journal*, 2006, **90**, 3012-3018.
10. J. Lee, A. A. Abdeen and K. A. Kilian, *Scientific reports*, 2014, **4**.
11. W. Zhao, X. Li, X. Liu, N. Zhang and X. Wen, *Materials Science and Engineering: C*, 2014, **40**, 316-323.
12. B. Trappmann, J. E. Gautrot, J. T. Connelly, D. G. Strange, Y. Li, M. L. Oyen, M. A. C. Stuart, H. Boehm, B. Li and V. Vogel, *Nature materials*, 2012, **11**, 642-649.
13. J. Li, D. Han and Y.-P. Zhao, *Scientific reports*, 2014, **4**.
14. O. Chaudhuri, S. T. Koshy, C. B. da Cunha, J.-W. Shin, C. S. Verbeke, K. H. Allison and D. J. Mooney, *Nature materials*, 2014, **13**, 970-978.
15. J. Ding, K. Ye, X. Wang, L. Cao, S. Li, Z. Li and L. Yu, *Nano letters*, 2015.
16. T.-Y. Huang, C.-H. Wu, M.-H. Wang, B.-S. Chen, L.-L. Chiou and H.-S. Lee, *BioMed Research International*, 2015, **2015**.
17. J. S. Park, J. S. Chu, A. D. Tsou, R. Diop, Z. Tang, A. Wang and S. Li, *Biomaterials*, 2011, **32**, 3921-3930.
18. A. K. Blakney, M. D. Swartzlander and S. J. Bryant, *Journal of biomedical materials research. Part A*, 2012, **100**, 1375.
19. A. Saez, M. Ghibaudo, A. Buguin, P. Silberzan and B. Ladoux, *Proceedings of the National Academy of Sciences*, 2007, **104**, 8281-8286.
20. E. Anon, X. Serra-Picamal, P. Hersen, N. C. Gauthier, M. P. Sheetz, X. Trepat and B. Ladoux, *Proceedings of the National Academy of Sciences*, 2012, **109**, 10891-10896.
21. Y. Wang, G. Wang, X. Luo, J. Qiu and C. Tang, *Burns*, 2012, **38**, 414-420.
22. X. Trepat, M. R. Wasserman, T. E. Angelini, E. Millet, D. A. Weitz, J. P. Butler and J. J. Fredberg, *Nature physics*, 2009, **5**, 426-430.
23. H. Zarkoob, S. Bodduluri, S. V. Ponnaluri, J. C. Selby and E. A. Sander, *Cellular and molecular bioengineering*, 2015, **8**, 32-50.
24. J. M. Goffin, P. Pittet, G. Csucs, J. W. Lussi, J.-J. Meister and B. Hinz, *The Journal of Cell Biology*, 2006, **172**, 259-268.
25. M. Brown, D. Adyshev, V. Bindokas, J. Moitra, J. G. Garcia and S. M. Dudek, *Microvascular research*, 2010, **80**, 75-88.
26. J. Lötters, W. Olthuis, P. Veltink and P. Bergveld, *Journal of Micromechanics and Microengineering*, 1997, **7**, 145.
27. A. Mata, A. J. Fleischman and S. Roy, *Biomedical microdevices*, 2005, **7**, 281-293.
28. O. Chaudhuri, L. Gu, M. Darnell, D. Klumpers, S. A. Bencherif, J. C. Weaver, N. Huebsch and D. J. Mooney, *Nature communications*, 2015, **6**.
29. Z. Wang, A. A. Volinsky and N. D. Gallant, *Journal of Applied Polymer Science*, 2014, **131**.
30. K.-S. Koh, J. Chin, J. Chia and C.-L. Chiang, *Micromachines*, 2012, **3**, 427-441.
31. R. N. Palchesko, L. Zhang, Y. Sun and A. W. Feinberg, 2012.
32. V. Vogel and M. Sheetz, *Nature Reviews Molecular Cell Biology*, 2006, **7**, 265-275.
33. B. Roy, T. Das, T. K. Maiti and S. Chakraborty, *Analytica chimica acta*, 2011, **701**, 6-14.
34. J. Wang, Y. Zhang, N. Zhang, C. Wang, T. Herrler and Q. Li, *Cellular and Molecular Life Sciences*, 2015, **72**, 2091-2106.
35. P. P. Provenzano and P. J. Keely, *Journal of Cell Science*, 2011, **124**, 1195-1205.
36. O. Huber, R. Korn, J. McLaughlin, M. Ohsugi, B. G. Herrmann and R. Kemler, *Mechanisms of development*, 1996, **59**, 3-10.
37. J. Behrens, J. P. von Kries, M. Kühl, L. Bruhn, D. Wedlich, R. Grosschedl and W. Birchmeier, *Nature*, 1996, **382**, 638-642.
38. H. Posthaus, L. Williamson, D. Baumann, R. Kemler, R. Caldelari, M. M. Suter, H. Schwarz and E. Müller, *Journal of Cell Science*, 2002, **115**, 4587-4595.
39. J. G. Wang, M. Miyazu, E. Matsushita, M. Sokabe and K. Naruse, *Biochemical and biophysical research communications*, 2001, **288**, 356-361.
40. J. G. Wang, M. Miyazu, P. Xiang, S. N. Li, M. Sokabe and K. Naruse, *Life sciences*, 2005, **76**, 2817-2825.
41. N. Wang, J. D. Tytell and D. E. Ingber, *Nature Reviews Molecular Cell Biology*, 2009, **10**, 75-82.
42. K. N. Dahl, A. J. Ribeiro and J. Lammerding, *Circulation research*, 2008, **102**, 1307-1318.
43. D. E. Discher, P. Janmey and Y.-l. Wang, *Science*, 2005, **310**, 1139-1143.

RSC Advances Accepted Manuscript

This journal is © The Royal Society of Chemistry 2015

Please do not adjust margins

44. J. Viac, S. Palacio, D. Schmitt and A. Claudy, *Archives of dermatological research*, 1997, **289**, 158-163.
45. G. Pagès and J. Pouysségur, *Cardiovascular research*, 2005, **65**, 564-573.
46. K. E. Derricks, V. Trinkaus-Randall and M. A. Nugent, *Integrative Biology*, 2015.

RSC Advances Accepted Manuscript

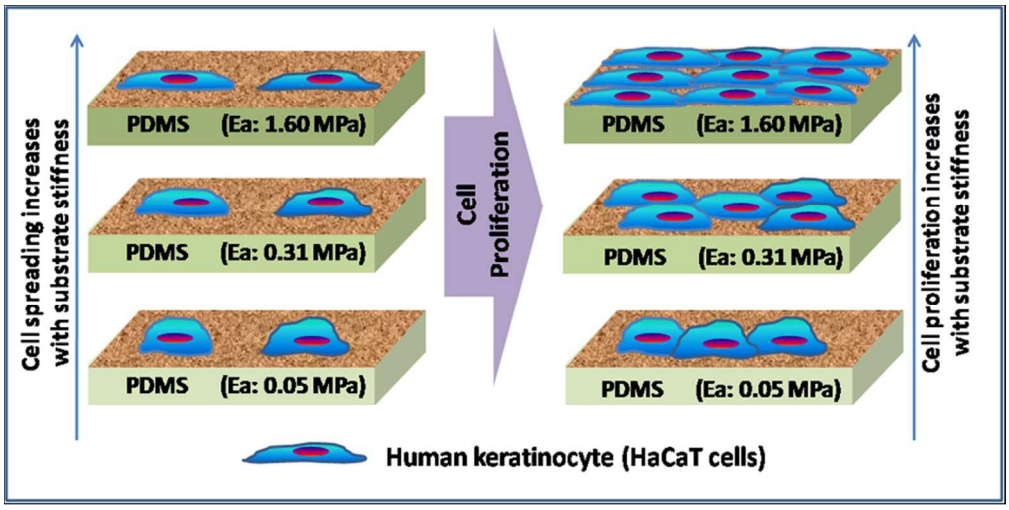

80x39mm (300 x 300 DPI)

RSC Advances Accepted Manuscript